PCCP
Physical Chemistry Chemical Physics

Accepted Manuscript

This article can be cited before page numbers have been issued, to do this please use: V. quintano, V. Diez-Cabanes, S. dell'Elce, L. Di Mario, J. S. Pelli Cresi, A. Paladini, D. Beljonne, A. Liscio and V. Palermo, *Phys. Chem. Chem. Phys.*, 2021, DOI: 10.1039/D1CP00740H.

View Article Online
DOI: 10.1039/D1CP00740H

ARTICLE

Measurement of conformational switching of azobenzenes from macro- to attomolar scale in self-assembled 2D and 3D nanostructures

ipaReceived 00th January 20xx,
Accepted 00th January 20xx

DOI: 10.1039/x0xx00000x

Vanesa Quintano,[a] Valentin Diez-Cabanes,[b] Simone Dell'Elce,[c] Lorenzo Di Mario,[d] Stefano Pelli Cresi,[d] Alessandra Paladini,[d] David Beljonne,[b] Andrea Liscio,[a]* Vincenzo Palermo.[a,e]*

It is important, but challenging, to measure the (photo) induced switching of molecules in different chemical environments, from solution, to thin layers, to solid bulk crystals. We compare the cis-trans conformational switching of commercial azobenzene molecules in different liquid and solid environments: polar solutions, liquid polymers, 2D nanostructures and 3D crystals. We achieve this goal using complementary techniques: optical absorption spectroscopy, femtosecond transient absorbance spectroscopy, Kelvin probe force microscopy and reflectance spectroscopy, supported by density functional theory calculations. We could observe the same molecule showing fast switching in few picoseconds, when studied as isolated molecule in water, or slow switching in tens of minutes, when assembled in 3D crystals. Noteworthy, we could also observe switching for small ensembles of molecules (few attomoles), representing an intermediate case between single molecules and bulk structures. This was achieved using Kelvin probe force microscopy to monitor the change of surface potential of nanometric thin 2D islands containing ca. 10^6 molecules each, self-assembled on a substrate. This approach is not limited to azobenzenes, but can be used to observe molecular switching in isolated ensembles of molecules or others nano-objects and to study synergic molecular processes at the nanoscale.

1. Introduction

Molecular switches are a class of molecules which are able to reversibly change their chemical structure upon the effect of certain stimuli such as light irradiation or change of the temperature.[1] They have been extensively studied for a wide range of applications, including solid-state electronics[2] molecular sensing,[3] thermal fuel storage,[4] or nanobiology,[5] thus attracting more and more interest from the scientific community, as confirmed by the Nobel Prize in Chemistry in 2016 awarded to Sauvage, Stoddart and Feringa "for the design and synthesis of molecular machines".[6]

Molecules with a central axis formed by a double bond are usually hindered rotors in the ground state, but they can also twist upon optical excitation, leading to a cis-trans isomerization.[7-9] In most cases, such conformational switching process occurs between two different well-defined states and is accompanied by the on/off switch of a certain property, which can be measured by a change in the electronic or optical absorption spectra, luminescence signals or nuclear magnetic resonance.[10]

One of the most well-known classes of molecular switches are azobenzenes (fig. 1). These molecules show photoisomerization from trans- to cis- conformation around the N=N bond by absorbing UV light, while returning to a trans conformation when they are exposed to visible light or heat.

This conformational switching can be easily observed in real time by using optical spectroscopy[11] and it can be ideally exploited in order to obtain a light-driven operation in molecular machines or smart materials.[12]

In particular, dyes featuring the azo linkage (-N=N-) are important for both fundamental studies and technological applications, due to their extensive use as dyes in the textile industry and colorant inks, and more recently due to their new applications in optical switching and optical data storage techniques.[13, 14]

The switching of azobenzenes has been vastly studied in solution, where macroscopic amounts of molecules can be studied by optical techniques.[15, 16] In an ideal case molecules are free from steric hindrance, isolated from one another and dispersed in a uniform medium. Even in such an ideal situation, the switching mechanisms may occur by following different reaction pathways, including direct N=N bond torsion, N center inversion or more complex coordinated movements of nitrogen and phenyl groups.[17-20] In addition, the switching process in

[a] Institute of Organic Synthesis and Photoreactivity (ISOF),– (CNR), via Gobetti 101, 40129 Bologna, Italy,
[b] Laboratory for Chemistry of Novel Materials, University of Mons, Place du Parc 20, B-7000 Mons, Belgium
[c] Graphene-XT srl, via D'Azeglio 15, 40123 Bologna, Italy,
[d] Division of Ultrafast Processes in Materials (FLASHit), Institute of Structure of Matter (ISM) – CNR, via del Fosso del Cavaliere 100, 00133 Rome, Italy,
[e] Institute for Microelectronics and Microsystems (IMM), National Research Council of Italy (CNR), via del Fosso del Cavaliere 100, 00133 Rome, Italy,
[f] Department of Industrial and Materials Science, Chalmers University of Technology, Hörsalvägen 7, 41296 Gothenburg, Sweden.
† Footnotes relating to the title and/or authors should appear here.
Electronic Supplementary Information (ESI) available: [details of any supplementary information available should be included here]. See DOI: 10.1039/x0xx00000x

solution is influenced by the solvent polarity and proticity, while the solvent viscosity seems to have a lower impact in the switching dynamics (see ref.[21] and references therein).

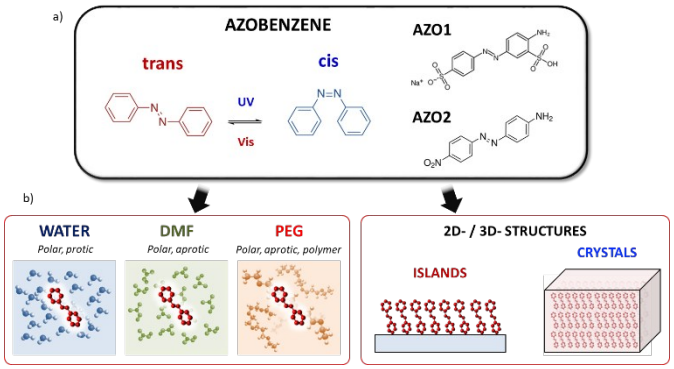

Fig. 1. a) Azobenzene: structure and different conformations. Molecules studied in this work: (AZO1) 2-Amino-5-([4-sulfophenyl] azo) benzenesulfonic acid (Acid yellow 9, CAS: 74543-21-8) and (AZO2) 4-(4-Nitrophenylazo) aniline (CAS: 730-40-5). b) Schematic representation of all the different solid and liquid environments where the cis → trans switching of the molecule was studied

While switching of azobenzenes in organic solvents can be easily studied for bulk solutions, most of their possible applications (e.g. in electronics) need to take place in solids or on surfaces, in a constrained environment, more challenging to be studied. Azobenzene is able in principle to isomerize even under the effect of strong constraints,[22, 23] such as the tight environments derived from solid matrices or from their inclusion in polymer chains.

As an example, some applications in electronics require the deposition of the azobenzenes on a 2D substrate, possibly in ordered, self-assembled monolayers.[24] In contrast, applications as industrial dyes require the dispersion of the azobenzenes in a 3D matrix (typically a polymer).

Switching of self-assembled monolayers (SAMs) based on azobenzene molecules has been already studied at macroscopic ensemble level by using spectroscopic techniques[22, 25-27] or at molecular level by means of microscopic or computational techniques.[21, 27] The influence of the environment on the isomerization of azobenzene in constrained confinements is still an important matter of debate in the community, and requires careful consideration when comparing various methods.[22]

Here, we present a complete experimental study on the properties of model azobenzene compounds focusing on how the cis-trans switching behaviour is influenced by the environment, in particular when the molecule is solubilized in different solvents, dispersed in polymers, deposited in 2D layers on a substrate or arranged in 3D crystals (fig. 1b). For this purpose, we had to overcome different limitations due to the solubility of the molecule, its processability and the complementary limitations of the different techniques used in this work. By combining spectroscopic studies in solution and on a surface with microscopic techniques, we observed the cis-trans switching of such azobenzene molecules both in bulk ensembles and in nanoscopic structures.

We chose two commercial azo compounds as target molecules: 2-Amino-5-([4-sulfophenyl] azo) benzenesulfonic acid (Acid yellow 9, CAS: 74543-21-8, Merck) named AZO1, and 4-(4-Nitrophenylazo) aniline (CAS: 730-40-5, Merck) named AZO2.

AZO1 is an aminoazobenzene-class molecule commercialized as a biological stain, and formerly used as a food dye (E105).[28] One of the two azobenzene rings is decorated with one sulfonic acid (Donor) and one amine (Acceptor) group, in meta- and para-positions respectively; while the other ring is substituted with a sulfonic acid sodium salt in a para- position.

Given the good solubility in a wide range of solvents due to the presence of two sulphonic groups we studied the switching behaviour of AZO1 in polar solvents: protic (water) and aprotic (dimethylformamide, DMF).

Previous works have suggested that solvent viscosity could have minimal influence on the switching rate of azobenzenes.[21, 29] Thus, besides small molecular solvents, we tested the switching behaviour of AZO1 also in a polymeric matrix environment, i.e. in Polyethylene glycol with average M_n = 400 (PEG). This liquid polymer, widely used in academy and industry, also provides a polar, aprotic environment for solvated molecules. PEG has significant polarity and a viscosity ≈90 mPa·s, two orders of magnitude higher than the one of water (0.89 mPa·s) and DMF (0.8 mPa·s).

AZO2 is a pseudostilbene-type molecule, a dye used in colouring natural and synthetic fabrics. It can be found in many clothing materials such as acetates, nylon, silk, wool, and cotton. This compound is a more conventional azobenzene bearing no charges, which possess an electron-donating NH_2 group on one phenyl ring, and an electron withdrawing NO_2 group on the other, with dipole moment = 14.08 D. The donor-acceptor asymmetric functionalization causes a strong charge transfer character to the π-π* transition (ca 390 nm), which is then red-shifted and overlaps the n-π* transition (ca 480 nm) – see fig. S2 for calculated spectra) – thus lowering the energy barrier between the cis and trans forms and making the switching process extremely easy at room temperature. Such molecule could thus be able to switch even in sterically hindered situations. Due to the lack of sulphonic groups, AZO2 is much less soluble than AZO1 and then it could not be processed in many solvents, including water. In this case, AZO2 could be solubilized in DMF solvent, where it showed ultra-fast switching, similarly to AZO1 in water.

2. Experimental

2.1 Materials

All the chemicals (solvents and azobenzene systems) were provided by Merck. Solvents: water HPLC, DMF 99.8% purity, and PEG average M_n = 400, (CAS number: 25322-68-3). Commercial azobenzene compounds: 2-Amino-5-([4-sulfophenyl] azo) benzenesulfonic acid (Acid yellow 9, CAS number: 74543-21-8) named AZO1, and 4-(4-Nitrophenylazo) aniline (CAS number: 730-40-5) named AZO2.

2.2 Sample preparation

DOI: 10.1039/D1CP00740H

The silicon wafers were treated with ultrasonication in ethanol and acetone for twenty minutes each before being dried in the oven.

2D nanostructures. AZO1 was dissolved in water (conc. = 10 mg/L). and AZO2 was dissolved DMF and THF, (conc. = 2 mg/L and conc. = 10 mg/L, respectively). The islands were obtained by drop casting on a silicon substrate or quartz plate before annealing at 180 °C for 14.

3D crystals. Both AZO1 and AZO2 molecules were drop cast on flat silicon substrates from THF and DMF solutions, (conc. = 1 g/L) in an air atmosphere with relative humidity ranging between 40%-50%, and the entire apparatus was maintained in the dark as far as practicable.

2.3 Methods

UV-vis spectroscopy. We performed the absorption spectroscopy measure in the UV–Vis region using Lambda 650 instrument from Perkin-Elmer. Spectra were acquired in the range 200-800 nm in air. We used Quartz cuvettes having an optical path of 1 cm. The photo-switching of the azobenzenes was measured in different solutions: water, DMF and PEG. We induced trans $\rightarrow$ cis photoswitching by exposing to ultra-violet light of λ = 365 nm (Power density of 3.2 mW/cm^2).[20] cis $\rightarrow$ trans switching was instead achieved with visible light of λ = 440 nm or λ = 520 nm (Power density of 0.56 mW/cm^2 and 2.4 mW/cm^2, respectively). We illuminated each sample for different time intervals until observing photosaturation. A thermal power sensor from Thorlabs was used to measure the light intensity on the sample surface. We used a heat filter between light source and sample, to avoid radiative heating.[30]

Reflectometry. The UV–Vis spectra of the solid samples were recorded in the diffuse reflectance mode on a spectrophotometer (Perkin-Elmer, Lambda 650) equipped with a 150 mm integrating sphere (same excitation wavelengths and power used in standard UV-vis spectroscopy, see above).

Femtosecond transient absorbance spectroscopy (FTAS). The pump and probe experiments were performed with a laser system consisting of a 800 nm, 1 kHz chirped pulse amplifier seeded by a Ti:Sa oscillator. The pump pulses (385 nm and 410 nm) were produced in an Optical Parametric Amplifier pumped by the amplifier. The probe is a white light supercontinuum (350-800 nm) generated in a commercial Transient Absorbance (TA) spectrometer (FemtoFrame II, IB Photonics), by focusing the 800 nm radiation of the amplifier into a rotating CaF_2 crystal. The optical layout of the TA spectrometer consisted of a split beam configuration in which 50% of the white light passes through the sample solution contained in a 1 mm static cell, while the remainder is used as a reference to account for pulse to pulse fluctuations in the white light generation. The pump pulse is focused (circular spot of diameter = 400 μm) onto the sample with an energy density of 280 μJ/cm^2. The spot diameter of the probe pulse is approximatively 150 μm, and its time delay with respect to the pump pulse is scanned in time by varying the length of its optical path.

The instrument response function (IRF) was measured to be approximately 50 fs. All measurements were performed in air at room temperature. More experimental details on the setup can be found in previous works.[31, 32]

Nanoscale characterization by scanning probe microscopy. Atomic Force Microscopy (AFM) and Kelvin Probe Force Microscopy (KPFM) measurements were performed in air with a Multimode 8 (Bruker) using Pt/Ir-coated cantilever silicon tips (k = 2.8 N/m, Bruker) with oscillating frequencies in the range between 60 and 90 kHz. AFM and KPFM images were acquired in the same measurement; a topographic line scan was first obtained by AFM operating in tapping mode, and then that same line was rescanned in lift mode with the tip raised to a lift height of 20 nm using the amplitude modulation (AM) mode. KPFM allowed to map the topography and electric surface potential of the sample with a voltage resolution of about 5 mV, whereas the lateral resolution was few tens of nanometers. KPFM can measure the transport and generation of charges in nanometric structures as described extensively in previous works.[33, 34] Raw AFM and KFPM data were treated by using histogram-flattening procedures[35] to remove the experimental artefacts because of the piezo scanners. AZO molecules were deposited on commercial native silicon oxide substrate (Si-Mat@).

Density functional theory calculations. Ground state properties and molecular geometries relaxations were calculated at Density Functional Theory (DFT) level of theory within the Becke, 3-parameter, Lee-Yang-Parr (B3LYP) functional[36] and 6-31G(d,p) basis set. The calculation of the excited state properties was done by means of Time-Dependent DFT (TD-DFT) calculations on the previously optimized structures. This functional and basis set have been successfully applied in the description of the excited states in similar azobenzene based compounds.[37, 38] The effects of the solvent were introduced in our calculations by the Polarizable Continuum Model (PCM).[39] All the theoretical calculations presented in this work were performed within Gaussian16 package program.[40]

3. Results and discussions

3.1 AZO photoisomerization in liquid

We first used Time-Dependent Density Functional Theory (DFT) calculations to estimate the relative stability and the opto-electronic properties of the individual cis and trans conformers of AZO1 in each solvent, to compare them with experimental absorption spectra (fig. 2).

The complete set of spectra and full numerical details are available in fig. S3 and tables S1-S2 in Supporting Information.

In standard azobenzenes the trans form is energetically most stable respect the cis- form in the majority of cases. The photoisomerization to the cis- form takes place upon UV light irradiation, while cis → trans thermal isomerization occurs spontaneously in the dark owing to the thermodynamic preference of the trans isomer. In addition to thermal isomerization, photoinduced cis → trans isomerization is also possible upon visible light irradiation.[41]

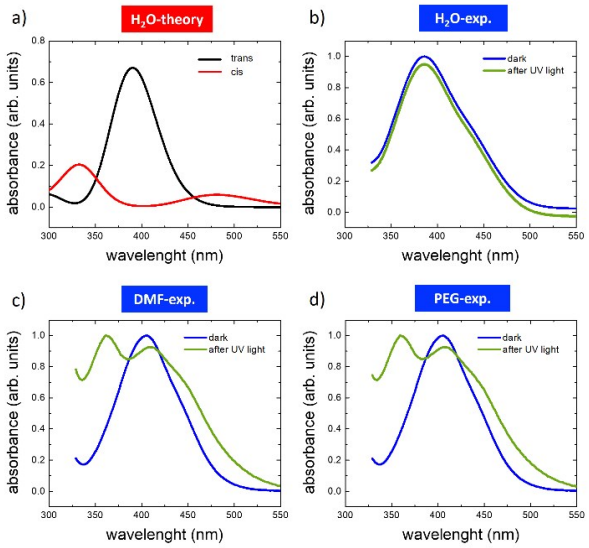

Fig. 2. Optical absorption spectra of AZO1 in different solvents. (a) Calculated TD-DFT spectra of the trans (red) and cis (black) isomers in water. Spectra measured before (blue) and after (green) UV illumination in (b) water, (c) DMF and (d) PEG. In the case of water the acquired curves have been Y-shifted to clearly distinguish them. The TD-DFT spectra for DMF and PEG are reported in Fig. S3.

DFT calculations predicted different absorption spectra for the *cis* and *trans* forms, while only a minor effect of the solvent environment was observed. In all the studied cases, the absorption spectra of the trans- form were dominated by an absorption peak centred between 300 and 400 nm due to the π–π* transition (see tables S1-S2). Upon illumination, a wide absorption peak was predicted between 300 and 400 nm assigned to the π–π* transition, and another at 450–500 nm assigned to the n–π* transition (see tables S1-S2). For the sake of simplicity, we depict only the simulation related to the water solvent (fig. 2a).

The experimental absorption spectra were acquired for each solution (fig.2 b-d) in the dark (blue curves) and after illumination with UV light, λ = 365 nm (green curves). In the dark, all azobenzene molecules were in the trans- configuration. In general, the calculations reproduced well the absorption spectra of the pristine trans form, showing only a small effect due to the solvent environment. The spectra measured on DMF were similar to those measured on PEG, both showing the main peak at ≈410 nm and a second one, not fully resolved, at ≈445 nm. Similar behaviour was observed in the case of water, where the main peak was shifted at ca 390 nm, while the second one, not fully resolved, was located in the region between 430 and 450 nm. These differences were attributed to the small effect of solvent on the HOMO-LUMO energies, which was directly affecting the band gap (see tables S1-S2). All the measurements were performed in a saturation regime, i.e. there is no dependence of the trans-cis switching rate on the photon flux.

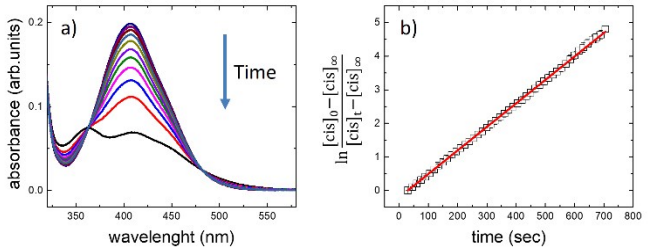

Fig. 3. (a) Changes in the absorption spectra of AZO1 in DMF upon irradiation at 365 nm. The arrow indicates the changes upon irradiation time. The different spectra have been recorded at 30 seconds time steps. (b) Kinetics of the isomerization. Absorbance at 410 nm (black squares) as a function of irradiation time. The red solid line shows a fit of the experimental data acquired during 5 cycles of irradiation under the same conditions.

Trans → cis isomerization was induced by light illumination at λ = 365 nm (Power density = 3.2 mW/cm^2) until no further spectral variation was observed, thus reaching the photostationary state (fig. 3) given by a mixture of both cis- and trans- isomers and defined by the experiment-specific balance between the UV-induced trans-cis isomerization and temperature-induced back (cis-trans) isomerization. Thereafter, we examined the backward (cis → trans) isomerization by turning off the 365 nm light source. The absorption spectra related to the back isomerization are reported in SI (fig. S3).

Table 1. Kinetic constants calculated for AZO1 switching in different solvents using eqn.1. Dielectric constants of the solvents, from literature and †calculated using eqn.2.

	k_+ (10^{-3} s^{-1})	k_- (10^{-3} s^{-1})	K (k_+ / k_-)	$\varepsilon_{solvent}$
PEG	150±20	45±0	3±1	12.4
PEG:H_2O (75%:25%)	100±50	40±5	2.5±0.6	27.8†
DMF	22±2	7.3±0.2	3.0±0.3	38.25
PEG:H_2O (50%:50%)	No switching observed	No switching observed	–	49.2†
PEG:H_2O (25%:75%)	No switching observed	No switching observed	–	69.2†
H_2O	No switching observed	No switching observed	–	80.1

At difference with the stationary absorption spectrum, the switching kinetics depended strongly on the polarity and proticity of the solvent used. In the case of DMF and PEG solvents, the formation of cis-AZO1 was clearly observed by the growth of a further peak at ca. 360 nm and the decrease of the

View Article Online
DOI: 10.1039/D1CP00740H

relative intensity of the peak at 410 nm, thus indicating the presence of a mixture of cis- and trans- isomers. However, no variations in the absorption spectrum were observed for AZO1 compound in water, where the optical absorption was stable upon prolonged illumination.

We used time-dependent measurements to estimate the kinetics of both the forward (trans → cis) and reverse (cis → trans) switching in the cases where the photoisomerization was observed, i.e. in DMF and PEG. The kinetic rate *k* of the forward (reverse) isomerization followed first-order kinetics (fig. 3b), and it was estimated following the same procedure as in previous azobenzene studies[42] by using the formula:

$$ln\frac{[cis]_0-[cis]_\infty}{[cis]_t-[cis]_\infty} = k\,t \qquad (1)$$

where $[cis]_0$, $[cis]_t$ and $[cis]_\infty$ are the concentrations of the cis-isomer at times 0, t and infinite, respectively; while *k* is the rate constant of the forward or reverse switching, corresponding to the slope of the linear trend measured in fig. 3b. [cis] value was estimated by measuring the absorption intensity at 410 nm. The calculated *k*-values for each solvent are reported in Table 1.

The kinetics of forward and reverse isomerization are intrinsically different. The isomerization rate constant of trans molecules (k_+) consists solely of the UV photon-induced mechanism, whereas for the reverse reaction of cis molecules (k_-) consists of thermal relaxation mechanisms.

We observed that: i) in both solvents, as soon as the UV-light exposure stops, AZO1 still remains largely in its *cis* state: $k_+ > k_-$, and ii) the photo-isomerization mechanisms occur slower in DMF than in PEG. Considering the case of water in which the molecule does not photo-switch (no transition rate, $k_{H2O} \cong 0$) we could write the follow hierarchy: $k_{+,PEG} > k_{+,DMF} > k_{+,H2O}$ ($k_{-,PEG} > k_{-,DMF} > k_{-,H2O}$). Taking into account that the rate of thermal-isomerization in non-polar solvents is faster than that in polar solvents,[43] our finding indicates the role of the solvent polarity in the photo-isomerization kinetics of AZO1, since the polarity index hierarchy is: PEG < DMF < H_2O.

While the rate constant values are different, their ratio is instead a constant. The equilibrium constant $K = k_+/k_-$ is the same for all the used solvents and amounts 2.9±0.1 clearly indicating that different solvents do not affect the electronic properties of azobenzene.

Such experimental result is confirmed by DFT calculations. The stabilization of AZO1 with the polarity of the solvent does not affect the frontier orbital (HOMO/LUMO) energies which are comparable for all three studied solvents (i.e. differences in energy between isomers range within 20 meV, see tables S1-S2). In particular, water is the solvent displaying the largest dielectric constant (ε_{H2O} = 80.1), thus being more effective than DMF (ε_{DMF} = 38.25) and PEG (ε_{PEG} = 12.4) for the stabilization of polar azobenzenes. However, this difference in the stability has a minor influence in the relative energy difference between trans- and cis- forms, which is about 0.62-0.64 eV in all cases. We underline that such theoretical description of the solvent is based on an explicit continuum model which is mainly dependent on the dielectric constant of the medium. Thus, no implicit effects (i.e. geometrical constraint) of the solvents are studied at this stage.

However, the case of water is more complex because of the role of hydrogen bond has to be taken into account together with the permittivity. The absence of any change in the absorption spectrum indicates that either AZO1 is so stable that it cannot switch ($k_{H2O} \cong 0$), or that the kinetics is faster than the temporal response of the experimental setup ($k_{H2O} >> 0$).

We faced such issue exploiting two different approaches: i) mixing solvents with different behaviors and ii) using ultra-fast spectroscopic techniques.

In the first case we mixed two solvents in which AZO1 shows opposite behaviors: PEG (observed switching) and H_2O (not observed switching) corresponding to five different mediums: ranging from pure water till pure PEG and with mixtures composed by 25%, 50% and 75% of PEG. Figure 4b depicts the variations of the optical absorption measured on the five systems as a function of the time turning ON/OFF the UV light (λ = 365 nm, irradiation time = 60 sec).

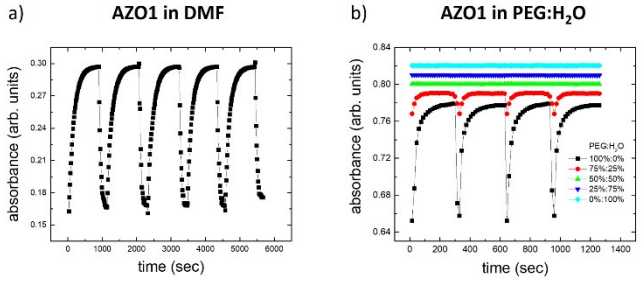

Fig. 4. Variation of optical absorption of AZO1 as a function of time in different solvents: a) DMF and b) five different mixtures of PEG:H_2O, ranging from pure water (0%:100%) till pure PEG (100%:0%).

A measurable switching was only observed with 75% of PEG, even if the absorbance variation ($abs_{cis}/abs_{trans} \approx 5\%$) was smaller than in the case of pure PEG ($abs_{cis}/abs_{trans} \approx 17\%$). Mixtures with lower amount of PEG did not show any switching behavior. All the rate constants are reported in Table 1.

The dielectric properties of such mixtures has been studied previously.[44] Due to the significant interaction between polyethylene glycols and water in the mixtures the effective permittivity (ε_{mix}) is not linearly dependent on the volume fraction of PEG (V_{PEG}). It follows instead a non-linear combination of the dielectric constants of the two solvents (ε_{PEG} and ε_{H2O}), described by the Bruggeman mixing formula[45] (see also ref.[46] and the references within for a comprehensive overview) and corrected by the structural rearrangement of the water molecules in the mixture, assuming the form:

$$\left[\frac{\varepsilon_{mix}-\varepsilon_{H2O}}{\varepsilon_{PEG}-\varepsilon_{H2O}}\right]\left[\frac{\varepsilon_{PEG}}{\varepsilon_{mix}}\right]^{1/3} = 1-[a-(a-1)(1-V_{PEG})]\cdot(1-V_{PEG}) \qquad (2)$$

where the parameter *a* contains the information regarding the change in the orientation of water molecules amounting. to 1.85 in PEG:H_2O mixtures.[44]

According to the eqn. 2 we calculated the dielectric permittivity values of the mixtures and we compared them with those of pure solvents.[47] All the values are reported in Table S1. We could note that the switching behavior caused by the UV light occurs when the dielectric constant of the solvent, being observed only when $\varepsilon_{solvent} \lesssim 40$. And indeed, the effective dielectric constant of the mixture with 75% PEG ($\varepsilon_{mix} = 27.8$) is closer to the dielectric constant of PEG respect the one of water. As expected, the equilibrium constant *K* measured on the mixture agrees with the values calculated on DMF and PEG.

It is important to underline that the observed phenomenological relationship between isomerization and effective dielectric constant of the solvent does not consider the role of OH, the effect of which is evinced in the case of isopropanol ($\varepsilon_{solvent} = 20$) showing an intermediate behavior between that observed in water and in DMF (fig. S5). Thus, the achieved relationship cannot be valid in the case of water due to the significant contribution of the hydrogen bonds. In general, the switching of sulfonic azobenzenes in an aqueous environment has been already demonstrated, meaning that the alcoholic groups of the azobenzene does not interfere by inhibiting the switching in water.[48]

All of these measurements were performed using conventional static UV-vis spectroscopy having a time resolution of a few seconds, which allowed to observe phenomena with kinetic constants $k_{\pm} < 1\ s^{-1}$. To overcome such issue we explored directly fast isomerization phenomena by means Femtosecond Transient Absorbance Spectroscopy (FTAS).

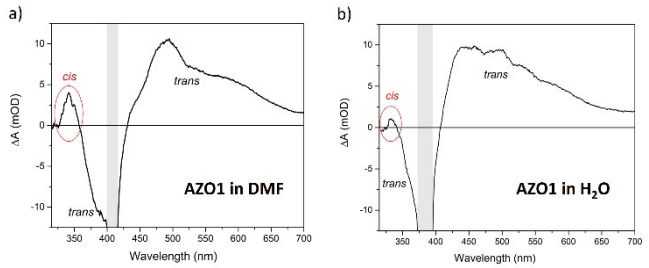

Fig. 5. Transient spectra of AZO1 in a) DMF and b) H_2O. The shaded areas show an intense negative feature due to scattered pump radiation around 410 nm and 385 nm, respectively. Energy density: 280 μJ/cm². The time delay between the pump and the probe is 0.65 ps.

We illuminated continuously a solution of AZO1 50 μM in DMF with UV light (λ = 365 nm) and then irradiated with a pump pulse at 410 nm, which corresponds to the maximum of the static absorption of the trans form (see fig. 2b). In analogy with the TA spectra of other azobenzene molecules,[49] the transient spectrum (see fig. 5a) clearly showed features due to the trans-form of AZO1. In particular, we observed positive signals in the range 450 – 750 nm (few picoseconds time decay) that could be assigned to excited state absorption and a negative signal around 380 nm (hundreds of picoseconds time decay) due to the ground state bleaching. A further weak positive signal is observed at 345 nm corresponding to photoinduced absorption from the vibration excited cis-AZO1, which was produced by the pump irradiation of the sample. It is expected that such signal was cut on the high energy side by the edge of the white light which screened the actual intensity of the signal. Analogous experiments were performed on a solution of AZO1, this time in water (100 μM) (see fig. 5b). Also, in this case the transient measurements seem to indicate that the trans → cis isomerization did take place, even if the efficiency was lower than in DMF, and the induced absorption signal of the cis product was less intense.

Although the kinetic rate was not directly measured (the estimated lower limit $k_{\pm} > 1\ s^{-1}$), FTAS measurements clearly show the presence of both cis and trans isomers of AZO1 both in water and DMF when illuminated with UV light confirming the photochromophore switching.

3.2 AZO photoisomerization in 2D nanostructures

In solution, molecules were isolated from each other and free to move (3 degrees of freedom of translational motion) and, as described above, the photoisomerization were mainly affected by the molecule – solvent interaction. Differently, when assembled in crystalline structures azobenzenes were fixed (no translational motion) and the photoisomerization were often much less efficient due to the close packing of molecules that limits structural changes.[50] We then explore an intermediate case where azobenzenes are constrained in 2D, forming demanding structures such as 2D assemblies created by depositing the molecules on a surface. In this case, molecules were not isolated, and their possible switching was hindered due to the interplay of molecule-molecule and molecule-surface interactions.[51]

We exploited thermodynamic effects to drive the self-assembly of azobenzene molecules to form micrometric islands and we directly observed the photoswitching of the single aggregate by means of two scanning probe microscopies: AFM and KPFM.

Techniques that allow the observation of molecular packing such as grazing-incidence small-angle X-ray scattering (GISAXS) or Scanning Tunneling Microscopy (STM) show some limitations for the study of single micrometric molecular aggregates. In the case of the first technique, the measurement is the average of different islands since the measurement area is larger than that of the single object, while the second generally requires a conductive substrate.

The use of scanning probe microscopies allows to overcome such issues. Although the AFM technique has no molecular resolution being typically < 5 nm (> 20 nm for KPFM), and therefore we cannot have direct information on the molecular packing, clear evidence on the arrangement could be provided by means histogram analysis.[35] Usually, a rough analysis of an AFM image is performed by studying a set of arbitrarily chosen profiles. Histogram analysis provided a complete description of the image in terms of 1D functions (i.e. Frequency Distribution of Height, FDH) consisting of the sum of all traced profiles allowing to calculate in a simple and direct way the thicknesses and roughness of the azobenzene nano-aggregates.

View Article Online
DOI: 10.1039/D1CP00749H

We performed the compared analysis of two azobenzene systems: AZO1 and AZO2 deposited on native silicon oxide with the same condition (see Methods).

Since there were no thiol groups or moieties interacting with substrate, we can neglect the interaction of azobenzenes with the superficial Si-OH sites of the substrate and point out the role of the molecule-molecule interaction. Moreover, due to good wettability of the fresh cleaned substrates, molecules can easily move on the surface self-aggregating, without remarkable kinetical constraining thanks to the slowly evaporation rate of the solvent.

Experimentally, the ΔSP value due to the photoswitching was calculated as the difference between the surface potential measured by KPFM after UV irradiation at 365 nm for 60 min and after visible light to restore the trans- configuration:

$$\Delta SP = KPFM_{UV} - KPFM_{vis}.$$

In the AZO1 case, we obtained well-defined islands with a lateral size of ca 1 μm and a uniform thickness h_{island} = 1.7±0.2 nm, as measured by AFM measurements (fig. 6a) performed on a statistic sample of 154 islands, clearly indicating that all the islands have the same molecule-molecule arrangement.

AZO1 is a polar salt, and the effective length of the azobenzene

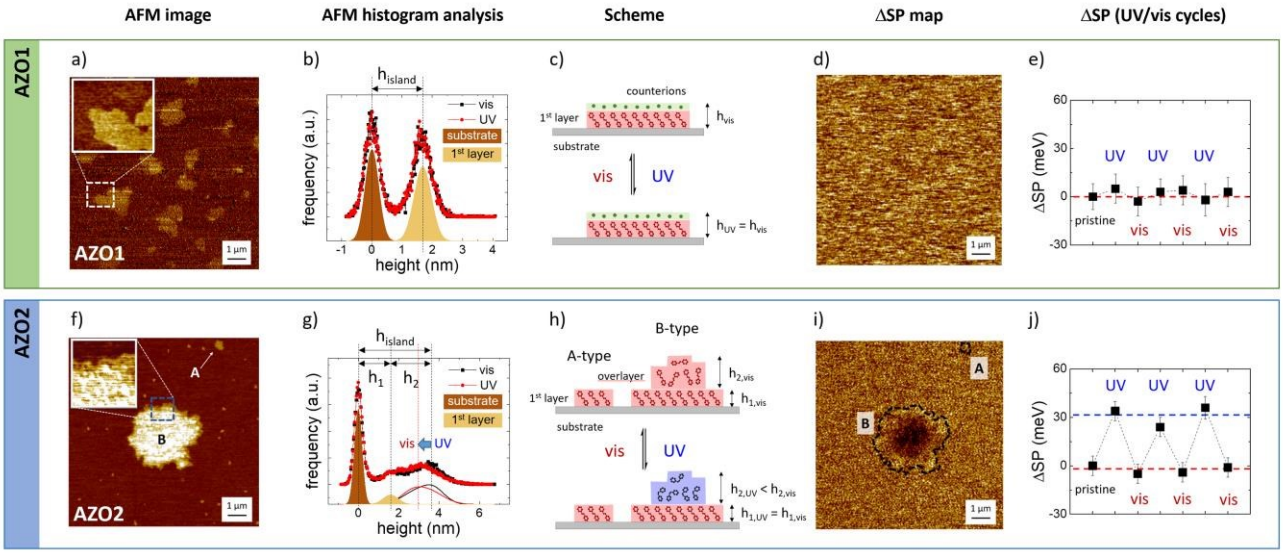

Fig. 6. AFM Morphology and corresponding KPFM Surface Potential maps on (a, d) AZO1 and (f, i) AZO2 islands deposited on silicon substrate. (b, g) Histogram analysis of the island edges reported in the two AFM image inserts acquired in vis- and UV- illumination. (c, h) Cartoon of the possible structure of the different islands before and after UV illumination. Time evolution of the surface potential ΔSP for (e) AZO1 and (i) AZO2, obtained by comparing SP values measured in the central part of the islands, as acquired after UV irradiation at 365 nm for 60 min and after visible light (436 nm) for further 60 minutes to restore the trans- configuration: $\Delta SP = KPFM_{UV} - KPFM_{vis}$. Measurements were repeated cycling UV and visible light. Z-ranges: (a, f) AFM images = 6 nm, (d, i) ΔSP images = 30 mV.

KPFM technique has been successfully applied to study *in-situ* changes in dipole moment in the monolayer,[52-54] where surface potential change is related to the dipole moment by the Helmholtz equation:[55]

$$\Delta SP_{cis \rightleftarrows trans} = \frac{1}{A\varepsilon_0\varepsilon_r}\left(\pm\mu_{z,trans} \mp \mu_{z,cis}\right) \qquad (3)$$

where $\mu_{z,cis/trans}$ is the vertical component of the dipole moment of cis and trans isomers, *A* is the average footprint of a typical azobenzene molecule, ε_0 and ε_r the dielectric constant of free space and the relative permittivity of the molecule.

In the case of disordered structure, eqn. 3 have to be modified taking into account all the molecular orientations in the aggregate preventing a direct solution. In general, disordered arrays of molecules show an intrinsic value of the measured dipole moment lower than that of ordered structures due to the average on all orientations of the molecules.

system is given by the molecular length (amounting ≈1.4 nm in trans- conformation, as estimated by Molecular Mechanics) and by surrounding Na^+ hydrated counter-ions with a diameter in solution of 0.72 nm (fig. 6c). Thus, in analogy with previous works, we could assume that the uniform thickness is due to the AZO1 molecule arranged in a tilted conformation surmounted by Na^+ ions and a significant amount of water molecules, being the measurements performed in air, as also suggested on AFM image by the presence of the strip along the direction of the moving of the scanning tip.

Inset figure in fig.6a represents the high-resolution image of the island edge, marked in the main image. The corresponding FDH (fig. 6b) reveals two main peaks corresponding to the substrate and the island where the thickness of the latter (h_{island}) is given by the distance between the two peaks commonly fitted with Gaussian curves. Moreover, the peak width is the root mean square roughness (R_{RMS}) of the corresponding nanostructure. R_{RMS} value measured on substrate peak amounts 0.36 nm, in excellent agreement with values reported in literature,[35]

proving the cleanliness of the substrate and the absence of experimental artifacts. In general, the variances of RRMS values were in the scale of 0.01 nm. For the sake of simplicity, RRMS values were reported with two significant digits without error.

AFM measurements were performed *in-situ* and no measurable variation is observed between the FDHs measured on single islands upon illumination at 365 nm for 60 min (red dots and line) and after vis illumination at 436 nm (black dots and line) to restore the trans-configuration. As well as the substrate, the R_{RMS} value of the AZO1 island did not vary when illuminated and amounts 0.4 nm (see SI for more details). Such findings clearly indicate that the molecules arrange themselves in ordered structures that are not modified by a light stimulus.

Similarly, no changes of surface potential could be observed by KPFM at the nanoscale: $\Delta SP = 1 \pm 3$ mV (fig. 6d) and repeating the vis/UV cycles for three times (fig. 6e).

In summary, the lack of switching measured in the AZO1 island has been attributed to different elements, or to their combination: i) the presence of counter-ions and charges that act as an electrical double layer, thus significantly shielding the variations of the dipole moment medium of the island due to switching and ii) tight packing of the molecules could hinder isomerization.

Thus, we performed the same measurement on a different molecule, AZO2 (fig. 6f, i) having a significant dipole moment (14.08 D) respect to the one of AZO1 (2.5 D).

In such case, we observed two different structures of AZO2 with different lateral sizes: (A) small islands with a lateral size up to 300 nm and uniform height $h_1 = 1.5 \pm 0.2$ nm, comparable to AZO2 length, and (B) large micrometric structures (up to 10 μm) with jagged edges and a height $h_1 = 1.6 \pm 0.2$ nm at the edges and a higher thickness up to 5 nm, in the central part of the island, as depicted of the zoom AFM image inset and the corresponding histogram analysis (fig. 6g). Such values have been determined on a set of 97 A-type and 14 B-type islands, corresponding to a total of about 1,000 μm^2 of scanned surface area.

The height of A-type islands suggests the presence of a single layer of azobenzene. Conversely, B-type islands show multi-layered structures with a first more ordered layer, visible at the islands' edge, surmounted by more disordered overlayers.

Histogram analysis revealed that A-type and first layer of B-type islands show the same root mean square roughness, $R_{RMS} = 0.2$ nm and, similarly to the case of AZO1, we did not observe any difference when samples were illuminated with visible or UV light. Conversely, the overlayers behaved differently as evinced by FDH measured during visible (black) or UV illumination (red). Focusing to the overlayer contribution (continuous lines), we clearly observed a change in the shape of the curves and a shift of the peak position of ca 0.7 nm. Take in account the variation of the shape (FDH is a weight function, see eqn. S2), we calculated that the average height of the overlayer drops by 0.4 nm when the sample is illuminated with UV light.

These findings confirmed the good structural order of the molecules forming the 1st layer, while AZO2 molecules were supported quite randomly in the overlayer.

In general, AZO2 shows a more complex self-assembly behavior than AZO1 due to the presence of two moieties ($-NH_2$ or $-NO_2$) that can bind to the substrate surface and interact differently with the solvent. Only in the case of DMF we could observe the reversible cis-trans switching at the nanoscale due to the changes in the KPFM signal. Fig. 6h shows the ΔSP map acquired on single islands of AZO2. While no significant modification of the topography was observed upon irradiation, a significant, reversible change of the surface potential $\Delta SP = 30 \pm 10$ mV was measured on single B-type islands. Instead, the potential of A-type structures showed no remarkable variation. KPFM images acquired before and after the illumination are reported in fig. S6). Moreover, the reversible change of the surface potential is measured in the B-type islands in correspondence with the wrinkled overlayer, while no change was measured in the well ordered first layer (or A-type island), suggesting that the structural disorder prevents steric constrains and allows the conformation switching of AZO2 molecules.

A further confirm of the role of the partial structural disorder was provided by the analysis of different self-assembled AZO2 structures obtained by using different solvents. The switching behavior of AZO2 could not be observed on well-ordered islands; KPFM measurements performed on different, fiber-like structures with flat surfaces, $R_{RMS} = 0.3$ nm (fig. S7, obtained by deposition from THF) did not show any observable switching.

The ΔSP measured in the AZO2 isolated islands is in agreement with previous measurements performed on continuous SAM layers,[53, 54] which though did not reach the single-island lateral resolution obtained here. This fact remarkably demonstrates that it is possible to measure the switching of small ensembles of molecules in real time. Assuming a typical island of 1×1 μm^2 and, an average footprint of a typical azobenzene molecule of ≈ 0.5 nm^2 obtained from STM measurements,[15] we could observe a clear and reversible switching of a small yet finite amount of molecules ($\approx 10^6$ molecules, or few attomoles). This result confirms the great potentiality of KPFM to measure molecular change of mesoscopic ensembles of molecules in real time, previously demonstrated on more disordered systems such as polymer chains or nanocrystals.[42, 44, 56]

3.3 AZO photoisomeriation in 3D crystals

Finally, we tried to monitor the cis-trans switching in 3D ordered structures. In general, coordinated switching of molecules in bulk solids is much more challenging than in solution or in nanostructures, due to the much stronger steric constrains, and the significant rearrangements needed to accommodate the new molecular packing; see as example the works of Feringa et al.[57] Koshima et al.[58] or Li et al.[59]

We were able to assemble 3D mesoscopic crystals for both AZO1 and AZO2 molecules on silicon substrates using standard solution processing, as depicted in fig. 7a,b. Both molecules assembled in large elongate crystals with typical dimensions of few tens of micron length, few hundreds of nanometers width and thickness ranging between 50 nm to 500 nm. The crystallinity of the structures was also supported by AFM measurements monitoring two features: the stepped surface and the roughness of the shelf of the step. In the first case, the crystal surface showed pits and steps of thickness ≈1.6 nm

Journal Name ARTICLE

(inset fig. 7a), comparable to the thickness of the AZO1 islands. The second feature indicated that the surface result as flat, R_{RMS} = 0.3±0.1 nm, as the substrate.

KPFM measurements on the surface of the micrometric crystals were intrinsically better resolved than in the case of nanostructures because of the lateral resolution. In particular, KPFM showed a small but significant change in the surface potential values measured before and after UV illumination: ΔSP was 5.8±0.4 mV and 4.6±0.4 mV, for AZO1 and AZO2, respectively, confirming the low efficiency of cis-trans switching in 3D systems respect to 2D islands or to isolated molecules in solution. It is noteworthy to underline that the measured ΔSP values agree with those achieved in 2D islands: AZO1 and 1st layer of AZO2, where the potential resolution is ca 10 meV.

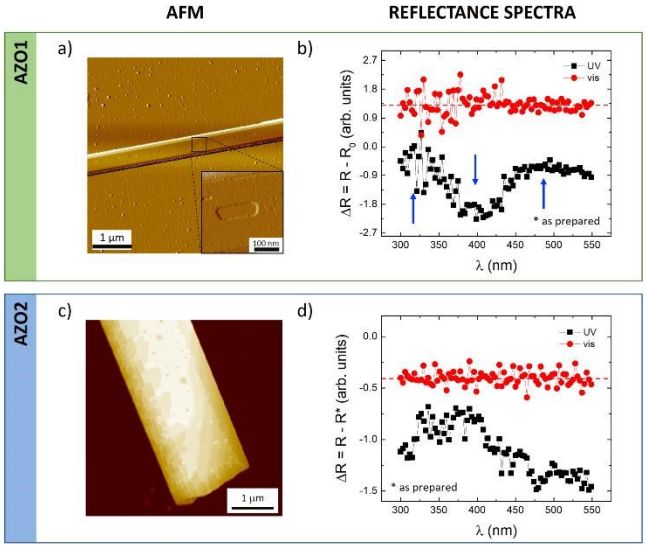

Fig. 7. (a, c) AFM images of corresponding (b,d) Reflectance spectra acquired on mesoscopic AZO1 and AZO2 crystals self-assembled on silicon (surface coverage < 5%). (a) phase AFM and (b) AFM morphology. Reflectance spectra ΔR given by the difference between the spectra measured after exposure to light and those obtained from non-irradiated samples (i.e. as prepared, R*). Black curve after 30 min exposure to UV light (λ = 365 nm, Power density = 3.2 mW/cm^2). Red curve after 30 min exposure to Vis light (λ = 440 nm, Power density = 0.56 mW/cm^2). Z-range: (a) arb. units, (c) 50 nm.

To confirm the KPFM values, we also compared them with optical reflectometry measurements which instead of measuring single islands measure the reflected light spectrum of the whole sample. Figure 7b,d reports the reflectance spectra ΔR obtained irradiated with UV (black) and visible (red) light, for both azobenzene molecules. All the spectra were obtained by subtracting the measurements collected from a non-irradiated samples, which had previously been stored in the dark (i.e. as prepared, R*), assuming that the film contained 100% trans azobenzene.

For both molecules we observed a similar behavior in the overall reflectance signals measured after UV and light illumination. Firstly, samples were irradiated with UV light for 30 min and reflectance spectra was recorded (black curve) showing a decrease close to 400 nm and an increase at ca 325 and ca 500 nm (marked with arrows for AZO1) corresponding to a partial conversion of trans- to cis isomerization, similarly to what has been observed previously.[60, 61] A following irradiation with visible light for 30 min revealed the opposite effect: the reflectance of the film (red line) became flat with irradiation time approaching to the curve measured on non-irradiated samples, confirming a recovery of the cis- isomers to the trans- counterparts.

It should be noted that reflectance spectra recorded on a reference film with no azobenzene showed no changes in the reflectance upon irradiation by UV or visible light (fig. S8), thus ruling out any artefact due to optical changes of the substrate upon illumination.

Both microscopic KPFM and macroscopic reflectance measurement thus confirm that cis → trans switching in 3D crystals can be observed, but is not very efficient in such 3D structures.

Conclusions

We measured the conformational switching of azobenzenes ranging from isolated molecules in liquid to attomolar- 2D and macro- scale 3D self-assembled structures.

Given the wide range of different environments, we used different complementary techniques. While optical steady-state spectroscopy is perfectly suited for conventional studies in solution, more refined techniques are needed to monitor switching featuring very fast or very slow kinetics. Although the FTAS spectroscopy measurements fail to monitor the switching, they are able to detect the presence of both the isomers also in case of very fast cis → trans switching confirming the photo-isomerization of both AZO molecules in all the tested liquid environments. Conversely, in case of constrained 2D micro-systems, scanning probe microscopies (AFM and KPFM) are a unique way to observe collective switching for relatively small ensembles (few attomoles, corresponding to ≈10^6 molecules) mapping the change of surface potential due to the dipole difference between cis- and trans- isomers.

When assembled in 2D and 3D aggregates we evinced the role of structural disorder by means of a quantitative analysis of AFM images. Reversible photoswitching was observed only in the case of disordered aggregates while ordered structures did not show remarkable variations.

This was confirmed by the measurements of ordered 3D structures, where switching is hindered due to steric constrains, but could also be observed with some specific techniques, as example macroscopic reflectometry measurements and, in best-case scenarios, with microscopic techniques such as KPFM. The possibility to compare the switching ability and time scale in ensembles with tunable amounts of these molecules could allow to better understand the effect of collective interactions to enhance and control their synergic switching. In particular, the design of partially ordered molecular structures could allow a suitable way to better enhance their performance in, as example, solid-state devices and thin coatings for electronics.

Conflicts of interest

There are no conflicts to declare.

Acknowledgements

This work was financially supported by the EC through the Marie Curie project ITN iSwitch (GA no. 642196), GrapheneCore2 (GA-785219), GrapheneCore 3 (GA-881603) projects – Graphene Flagship and from the Swedish Research Council under project (project Janus 2017-04456). Computational resources were provided by the Consortium des Équipements de Calcul Intensif (CÉCI) funded by the Belgian National Fund for Scientific Research (F.R.S.-FNRS) under Grant 2.5020.11. D.B. is a FNRS research director.

Notes and references

1. B. L. Feringa and W. R. Browne, *Molecular switches*, Wiley-VCH, Weinheim, Germany, 2nd, completely rev. and enl. edn., 2011.
2. E. Orgiu and P. Samori, *Advanced Materials*, 2014, **26**, 1827-1845.
3. Y. Shiraishi, S. Sumiya and T. Hirai, *Chemical Communications*, 2011, **47**, 4953-4955.
4. B. Champagne, A. Plaquet, J. L. Pozzo, V. Rodriguez and F. Castet, *Journal of the American Chemical Society*, 2012, **134**, 8101-8103.
5. M. Natali and S. Giordani, *Chemical Society Reviews*, 2012, **41**, 4010-4029.
6. J.-P. Sauvage and V. Amendola, *Molecular machines and motors*, Springer, Berlin ; New York, 2001.
7. H. Iwamura and K. Mislow, *Accounts of Chemical Research*, 1988, **21**, 175-182.
8. K. Kinbara and T. Aida, *Chemical Reviews*, 2005, **105**, 1377-1400.
9. G. S. Kottas, L. I. Clarke, D. Horinek and J. Michl, *Chemical Reviews*, 2005, **105**, 1281-1376.
10. V. Balzani, M. Gomez-Lopez and J. F. Stoddart, *Accounts of Chemical Research*, 1998, **31**, 405-414.
11. H. M. D. Bandara and S. C. Burdette, *Chemical Society Reviews*, 2012, **41**, 1809-1825.
12. V. Balzani, A. Credi and M. Venturi, *Chemical Society Reviews*, 2009, **38**, 1542-1550.
13. M. Min, S. Seo, S. M. Lee and H. Lee, *Advanced Materials*, 2013, **25**, 7045-7050.
14. K. G. Yager and C. J. Barrett, *Journal of Photochemistry and Photobiology a-Chemistry*, 2006, **182**, 250-261.
15. I. K. Lednev, T. Q. Ye, P. Matousek, M. Towrie, P. Foggi, F. V. R. Neuwahl, S. Umapathy, R. E. Hester and J. N. Moore, *Chemical Physics Letters*, 1998, **290**, 68-74.
16. E. M. M. Tan, S. Amirjalayer, S. Smolarek, A. Vdovin, F. Zerbetto and W. J. Buma, *Nature Communications*, 2015, **6**.
17. H. Dürr and H. Bouas-Laurent, *Photochromism : molecules and systems*, Elsevier, Amsterdam ; Boston, Rev. edn., 2003.
18. H. Rau and E. Luddecke, *Journal of the American Chemical Society*, 1982, **104**, 1616-1620.
19. T. Schultz, J. Quenneville, B. Levine, A. Toniolo, T. J. Martinez, S. Lochbrunner, M. Schmitt, J. P. Shaffer, M. Z. Zgierski and A. Stolow, *Journal of the American Chemical Society*, 2003, **125**, 8098-8099.
20. G. Tiberio, L. Muccioli, R. Berardi and C. Zannoni, *Chemphyschem*, 2010, **11**, 1018-1028.
21. M. Quick, A. L. Dobryakov, M. Gerecke, C. Richter, F. Berndt, I. N. Ioffe, A. A. Granovsky, R. Mahrwald, N. P. Ernsting and S. A. Kovalenko, *Journal of Physical Chemistry B*, 2014, **118**, 8756-8771.
22. T. Moldt, D. Przyrembel, M. Schulze, W. Bronsch, L. Boie, D. Brete, C. Gahl, R. Klajn, P. Tegeder and M. Weineltt, *Langmuir*, 2016, **32**, 10795-10801.
23. H. Rau and Y. Q. Shen, *Journal of Photochemistry and Photobiology a-Chemistry*, 1988, **42**, 321-327.
24. H. T. Zhang, X. F. Guo, J. S. Hui, S. X. Hu, W. Xu and D. B. Zhu, *Nano Letters*, 2011, **11**, 4939-4946.
25. V. Ferri, M. Elbing, G. Pace, M. D. Dickey, M. Zharnikov, P. Samori, M. Mayor and M. A. Rampi, *Angewandte Chemie-International Edition*, 2008, **47**, 3407-3409.
26. D. Ishikawa, E. Ito, M. N. Han and M. Hara, *Langmuir*, 2013, **29**, 4622-4631.
27. G. Pace, V. Ferri, C. Grave, M. Elbing, C. von Hanisch, M. Zharnikov, M. Mayor, M. A. Rampi and P. Samori, *Proceedings of the National Academy of Sciences of the United States of America*, 2007, **104**, 9937-9942.
28. S. Das, P. V. Kamat, S. Padmaja, V. Au and S. A. Madison, *Journal of the Chemical Society-Perkin Transactions 2*, 1999, DOI: 10.1039/a809720h, 1219-1223.
29. C. W. Chang, Y. C. Lu, T. T. Wang and E. W. G. Diau, *Journal of the American Chemical Society*, 2004, **126**, 10109-10118.
30. C. Weber, T. Liebig, M. Gensler, A. Zykov, L. Pithan, J. P. Rabe, S. Hecht, D. Bleger and S. Kowarik, *Scientific Reports*, 2016, **6**.
31. P. O'Keeffe, D. Catone, A. Paladini, F. Toschi, S. Turchini, L. Avaldi, F. Martelli, A. Agresti, S. Pesceteli, A. E. D. Castillo, F. Bonaccorso and A. Di Carlo, *Nano Letters*, 2019, **19**, 684-691.
32. F. Toschi, D. Catone, P. O'Keeffe, A. Paladini, S. Turchini, J. Dagar and T. M. Brown, *Advanced Functional Materials*, 2018, **28**.
33. A. Liscio, V. Palermo and P. Samori, *Advanced Functional Materials*, 2008, **18**, 907-914.
34. A. Liscio, V. Palermo and P. Samori, *Accounts of Chemical Research*, 2010, **43**, 541-550.
35. A. Liscio, *Chemphyschem*, 2013, **14**, 1283-1292.
36. A. D. Becke, *Journal of Chemical Physics*, 1993, **98**, 1372-1377.
37. D. Bleger, J. Dokic, M. V. Peters, L. Grubert, P. Saalfrank and S. Hecht, *Journal of Physical Chemistry B*, 2011, **115**, 9930-9940.
38. J. Dokic, M. Gothe, J. Wirth, M. V. Peters, J. Schwarz, S. Hecht and P. Saalfrank, *Journal of Physical Chemistry A*, 2009, **113**, 6763-6773.
39. J. Tomasi, B. Mennucci and R. Cammi, *Chemical Reviews*, 2005, **105**, 2999-3093.
40. M. Frisch, G. Trucks, H. Schlegel, G. Scuseria, M. Robb, J. Cheeseman, G. Scalmani, V. Barone, G. Petersson and H. Nakatsuji, *Journal*, 2016.
41. N. K. Joshi, M. Fuyuki and A. Wada, *Journal of Physical Chemistry B*, 2014, **118**, 1891-1899.

Journal Name ARTICLE

View Article Online
DOI: 10.1039/D1CP00740H

42. T. Asano and T. Okada, *Journal of Organic Chemistry*, 1984, **49**, 4387-4391.
43. L. Zhou, L. Chen, G. Ren, Z. Zhu, H. Zhao, H. Wang, W. Zhang and J. Han, *Physical Chemistry Chemical Physics*, 2018, **20**, 27205-27213.
44. C. S. Mali, S. D. Chavan, K. S. Kanse, A. C. Kumbharkhane and S. C. Mehrotra, *Indian Journal of Pure & Applied Physics*, 2007, **45**, 476-481.
45. D. A. G. Bruggeman, *Annalen der Physik*, 1935, **416**, 636-664.
46. V. A. Markel, *Journal of the Optical Society of America a-Optics Image Science and Vision*, 2016, **33**, 1244-1256.
47. P. W. Atkins and J. De Paula, *Atkins' Physical chemistry*, Oxford University Press, Oxford ; New York, Tenth edition. edn., 2014.
48. S. Loudwig and H. Bayley, *Journal of the American Chemical Society*, 2006, **128**, 12404-12405.
49. J. Bahrenburg, K. Rottger, R. Siewertsen, F. Renth and F. Temps, *Photochemical & Photobiological Sciences*, 2012, **11**, 1210-1219.
50. A. Gonzalez, E. S. Kengmana, M. V. Fonseca and G. G. D. Han, *Materials Today Advances*, 2020, **6**, 100058.
51. G. M. Whitesides and M. Boncheva, *Proceedings of the National Academy of Sciences of the United States of America*, 2002, **99**, 4769-4774.
52. V. Palermo, M. Palma and P. Samori, *Advanced Materials*, 2006, **18**, 145-164.
53. B. Stiller, G. Knochenhauer, E. Markava, D. Gustina, I. Muzikante, P. Karageorgiev and L. Brehmer, *Materials Science & Engineering C-Biomimetic and Supramolecular Systems*, 1999, **8-9**, 385-389.
54. S. Schuster, M. Füser, A. Asyuda, P. Cyganik, A. Terfort and M. Zharnikov, *Physical Chemistry Chemical Physics*, 2019, **21**, 9098-9105.
55. D. Schuhmann, *Journal of Colloid and Interface Science*, 1990, **134**, 152-160.
56. A. Sihvola, *Subsurface Sensing Technologies and Applications*, 2000, **1**, 393-415.
57. J. W. Chen, F. K. C. Leung, M. C. A. Stuart, T. Kajitani, T. Fukushima, E. van der Giessen and B. Feringa, *Nature Chemistry*, 2018, **10**, 132-138.
58. H. Koshima, N. Ojima and H. Uchimoto, *Journal of the American Chemical Society*, 2009, **131**, 6890-+.
59. Y. F. Wang, S. Chen, L. Qiu, K. Wang, H. T. Wang, G. P. Simon and D. Li, *Advanced Functional Materials*, 2015, **25**, 126-133.
60. M. Moniruzzaman, P. Christogianni and G. Kister, in *Proceeding of 4th International Conference on Process Engineering and Advanced Materials*, eds. M. A. Bustam, Z. Man, L. K. Keong, A. A. Hassankiadeh, Y. Y. Fong, M. Ayoub, M. Moniruzzaman and P. Mandal, 2016, vol. 148, pp. 114-121.
61. M. Moniruzzaman, C. J. Sabey and G. F. Fernando, *Macromolecules*, 2004, **37**, 2572-2577.